Aerobic deconstruction of cellulosic biomass by an insect-associated *Streptomyces*

Taichi E. Takasuka[1,2,*], Adam J. Book[1,3,*], Gina R. Lewin,[1,3] Cameron R. Currie[1,3], and Brian G. Fox[1,2]

[1]DOE Great Lakes Bioenergy Research Center, [2]Department of Biochemistry, and [3]Department of Bacteriology, University of Wisconsin-Madison, Madison, Wisconsin, United States of America. *These authors contributed equally to this work. Correspondence and requests for materials should be addressed to C.R.C. (email: currie@bact.wisc.edu) or B.G.F. (email: bgfox@biochem.wisc.edu).

Supplementary Information

Figure S1 : Scanning electron microscopy images of ActE grown on different carbon sources including glucose, cellulose, xylan, switchgrass, ammonia ammonia fiber expansion-treated switchgrass (AFEX-SG) and ionic liquid-treated switchgrass (IL-SG). ActE cells were grown in minimum medium with the indicated substrate as a sole carbon source for 7 days at 30 ˚C. The scale bar indicates 5 μm.

Figure S2 : Fractionation of the ActE cellulose secretome and assays of reactions with different polysaccharides. (A) Anion exchange chromatography

was performed using the ActE cellulose secretome, and fractions were collected and analyzed by SDS-PAGE. Lowercase letters indicate protein identified by MALDI-TOF MS shown in Supplementary Table S1. (B) Results from hydrolysis assays for reaction with filter paper (FP), xylan, mannan and beta-1,3 glucan as detected by DNS assay of each fraction. The percentage reactivity relative to the maximum activity observed for each substrate is shown. Error bars indicate the standard deviation, with n = 3 for technical replicates.

Figure S3 : Temperature and pH profiles of the ActE secretome obtained from growth on AFEX-treated corn stover. (A) The effect of temperature on the deconstruction of AFEX-treated switchgrass (AFEX-SG) and ionic liquid-treated switchgrass (IL-SG). The relative activity of the ActE secretome was compared to the maximal rates determined for reaction with AFEX-SG (*blue star*), and IL-SG (*red star*) at pH 6.0. (B) The effect of pH on the AFEX-SG and IL-SG deconstruction activities in the indicated ActE secretomes. The maximal rates observed for AFEX-SG and IL-SG were at pH 7.0 (*blue star*) and pH 8 (*red star*), respectively. Reactions were carried out at 40 ˚C and the 0.1 M buffers used were citrate (pH 4.5), phosphate (pH 6-8), CHES (pH 9-10), and CAPS (pH 11). The reaction was performed for 20 h and the reducing sugar content was measured by DNS assay.

Figure S4 : Genome-wide changes in expression during growth of ActE on substrate cellobiose versus glucose visualized as a Cytoscape interaction

network. Nodes are genes (*circles*) or KEGG/CAZy functional categories (*yellow triangles*); edges indicate that the gene belongs to the indicated functional group as defined by either KEGG or CAZy analysis. Gene node sizes reflect expression intensity determined by microarray from growth on substrate as a $\log_2$ ratio. Node colors represent expression changes as the $\log_2$ ratio of substrate/glucose transcript intensities, where the genome-wide average transcriptional intensity was ~10.5 for both substrate and glucose. Transcripts with less than two-fold changes in expression intensity are colored white; transcripts with greater than two-fold increase in expression intensity during growth on substrate are shown as a red gradient; transcripts with greater than two-fold increase in expression intensity during growth on glucose are shown as a blue gradient.

Figure S5 : Genome-wide expression changes for growth on the substrate cellulose versus glucose visualized as a Cytoscape interaction network. Other information provided in the caption to Supplementary Fig. S4.

Figure S6 : Genome-wide expression changes for growth on the substrate xylan versus glucose visualized as a Cytoscape interaction network. Other information provided in the caption to Supplementary Fig. S4.

Figure S7 : Genome-wide expression changes for growth on the substrate switchgrass versus glucose visualized as a Cytoscape interaction network. Other information provided in the caption to Supplementary Fig. S4.

Figure S8 : Genome-wide expression changes for growth on the substrate IL-treated switchgrass versus glucose visualized as a Cytoscape interaction network**.** Other information provided in the caption to Supplementary Fig. S4.

Figure S9 : Genome-wide expression changes for growth on the substrate chitin versus glucose visualized as a Cytoscape interaction network. Other information provided in the caption to Supplementary Fig. S4.

Figure S10 : Expression of 167 predicted CAZy genes in ActE, highlighting group 2 genes. These genes showed no signal above the average genomic expression intensity (log_2 = 10.5). (A) Clustering of genes with similar expression profiles. (B) Additional information on group 2 genes including expression profile, SACTE_locus ID, CAZy family, and annotated function.

Figure S11 : Expression of 167 predicted CAZy genes in ActE, highlighting group 3 genes. (A) Clustering of genes with similar expression profiles. (B) Additional information on group 3 genes including expression profile, SACTE_locus ID, CAZy family, and annotated function.

Table S1 : Proteins separated by ion exchange chromatography and identified by mass spectrometry.

Figure S1

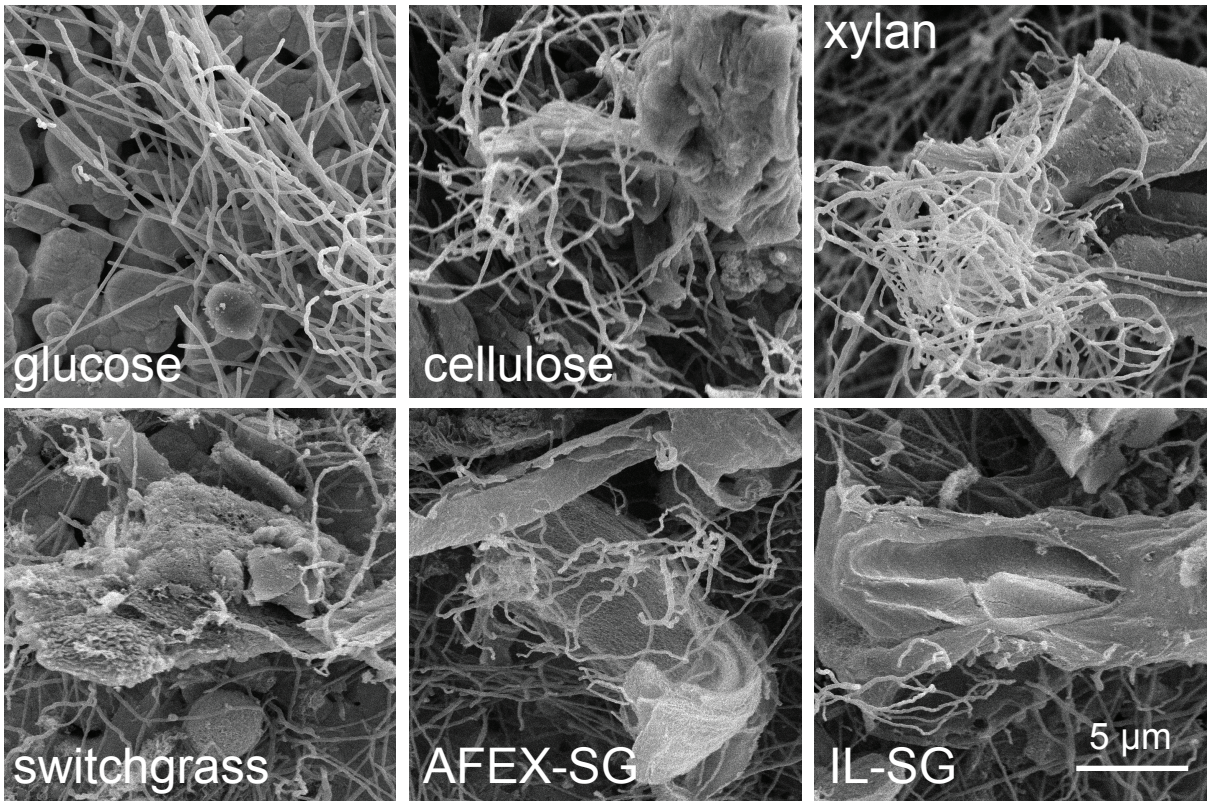

Figure S2

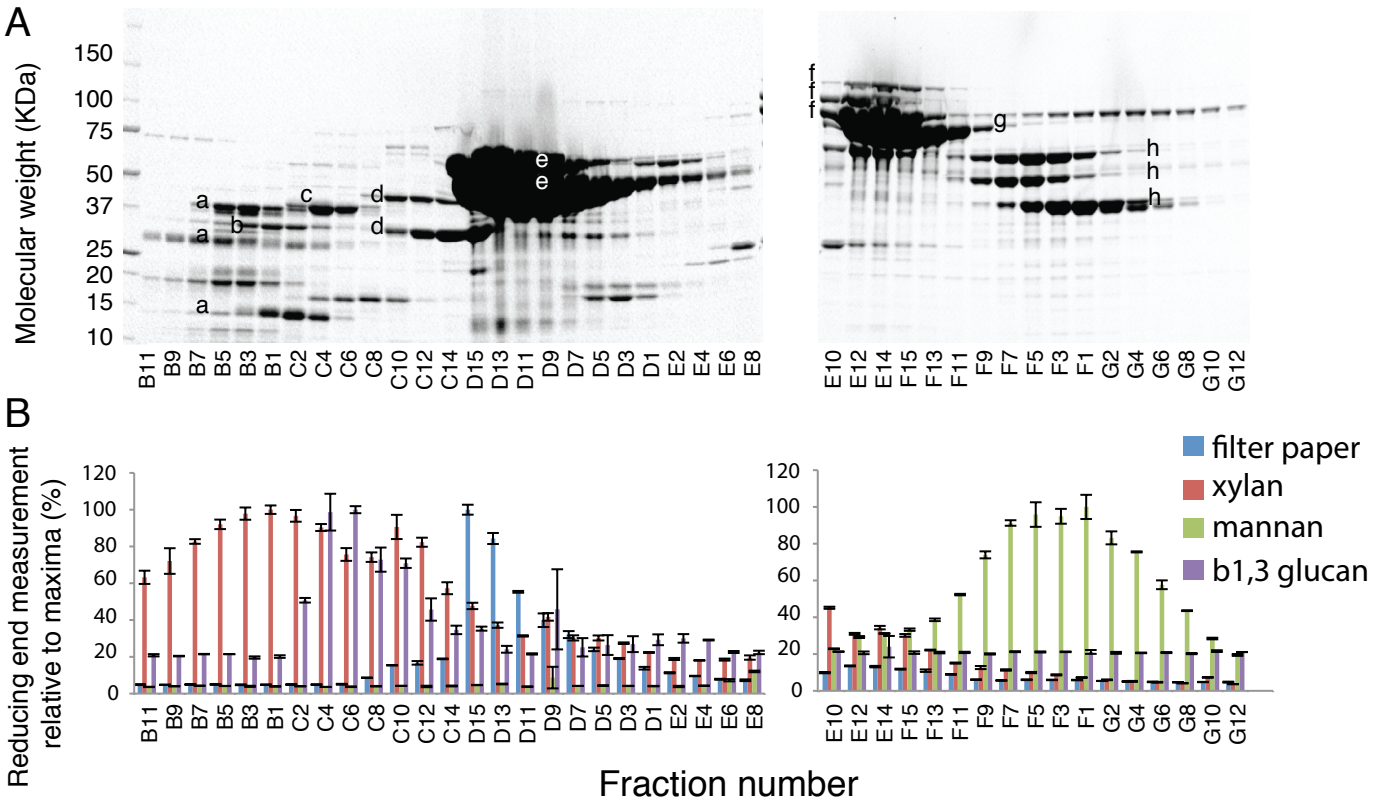
A
Molecular weight (KDa)
150
100
75
50
37
25
20
15
10
a
a
a
b
c
d
d
e
e
f
f
f
g
h
h
h
B11 B9 B7 B5 B3 B1 C2 C4 C6 C8 C10 C12 C14 D15 D13 D11 D9 D7 D5 D3 D1 E2 E4 E6 E8
E10 E12 E14 F15 F13 F11 F9 F7 F5 F3 F1 G2 G4 G6 G8 G10 G12
B
Reducing end measurement relative to maxima (%)
120
100
80
60
40
20
0
filter paper
xylan
mannan
b1,3 glucan
Fraction number

Figure S3

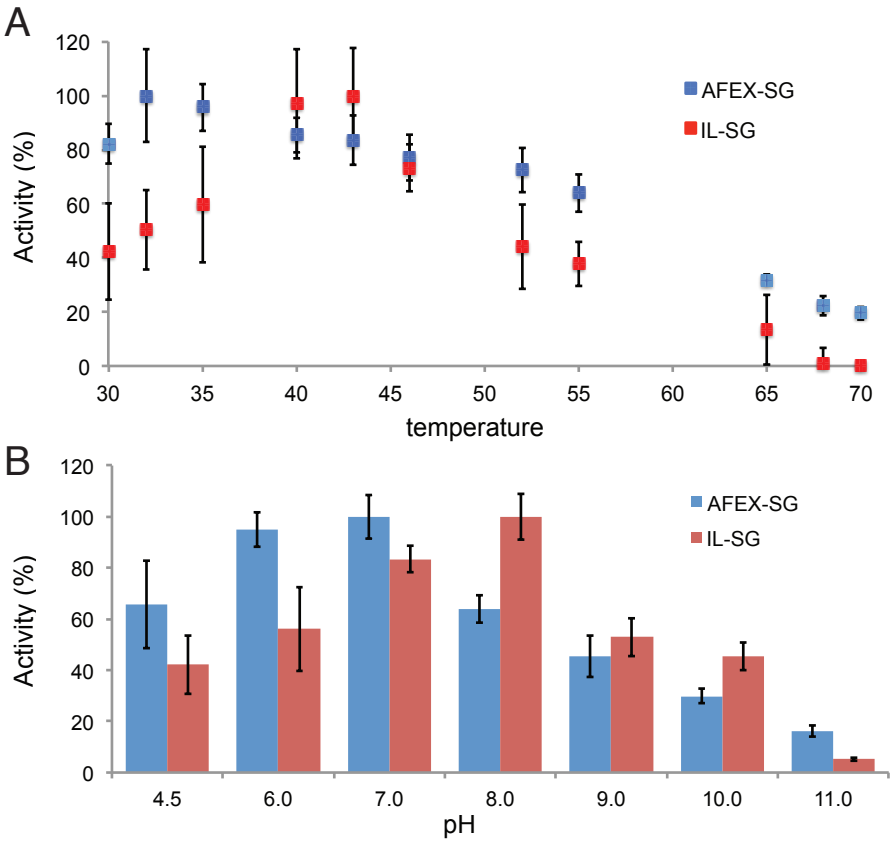
A
120
100
80
60
40
20
0
Activity (%)
30
35
40
45
50
55
60
65
70
temperature
AFEX-SG
IL-SG
B
120
100
80
60
40
20
0
Activity (%)
4.5
6.0
7.0
8.0
9.0
10.0
11.0
pH
AFEX-SG
IL-SG

Figure S4

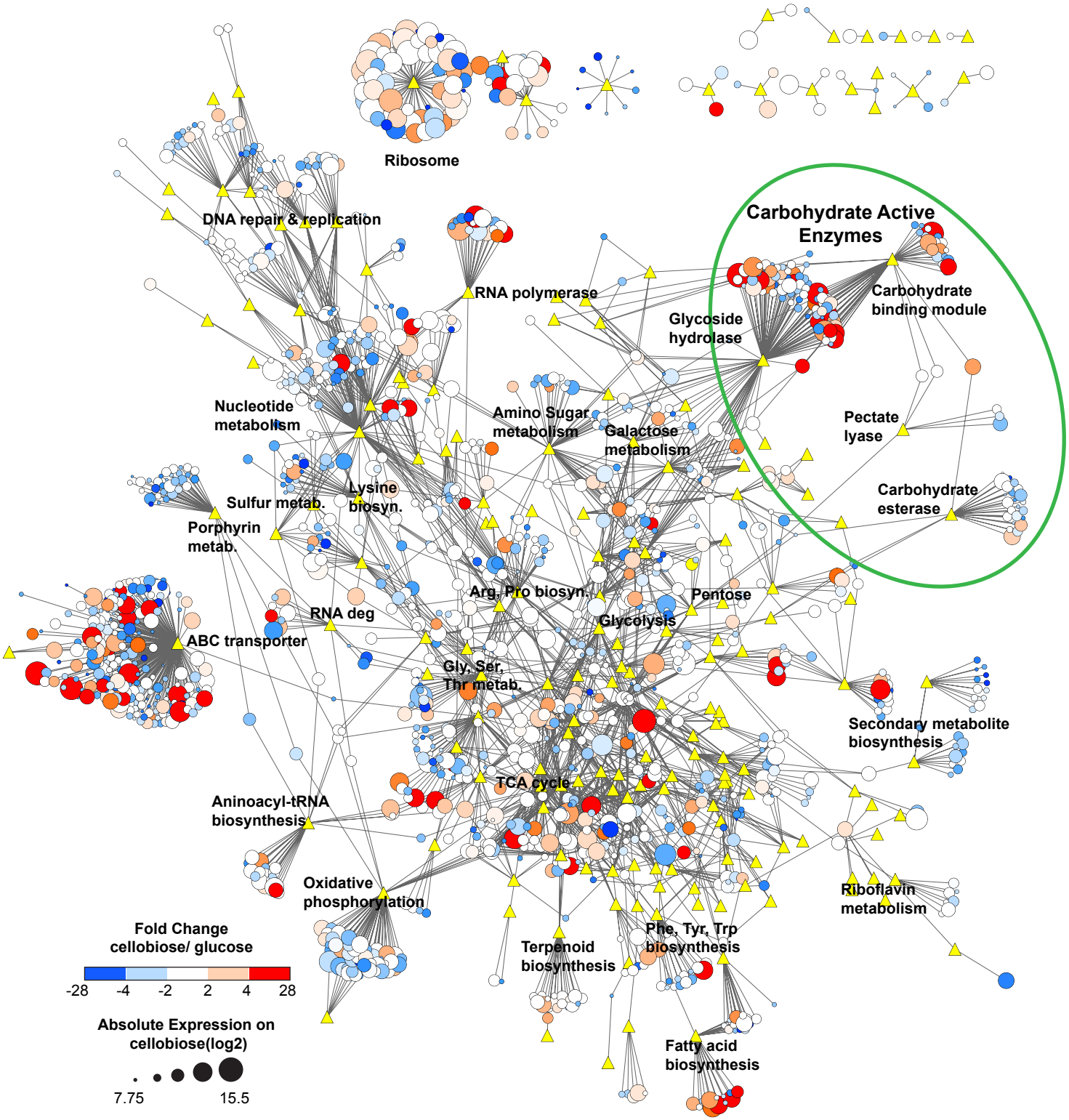
Ribosome
DNA repair & replication
RNA polymerase
Carbohydrate Active Enzymes
Carbohydrate binding module
Glycoside hydrolase
Nucleotide metabolism
Amino Sugar metabolism
Galactose metabolism
Pectate lyase
Carbohydrate esterase
Lysine biosyn.
Sulfur metab.
Porphyrin metab.
Arg, Pro biosyn.
Pentose
Glycolysis
RNA deg
ABC transporter
Gly, Ser, Thr metab.
Secondary metabolite biosynthesis
TCA cycle
Aninoacyl-tRNA biosynthesis
Oxidative phosphorylation
Riboflavin metabolism
Terpenoid biosynthesis
Phe, Tyr, Trp biosynthesis
Fatty acid biosynthesis
Fold Change cellobiose/ glucose
-28 -4 -2 2 4 28
Absolute Expression on cellobiose(log2)
7.75 15.5

Figure S5

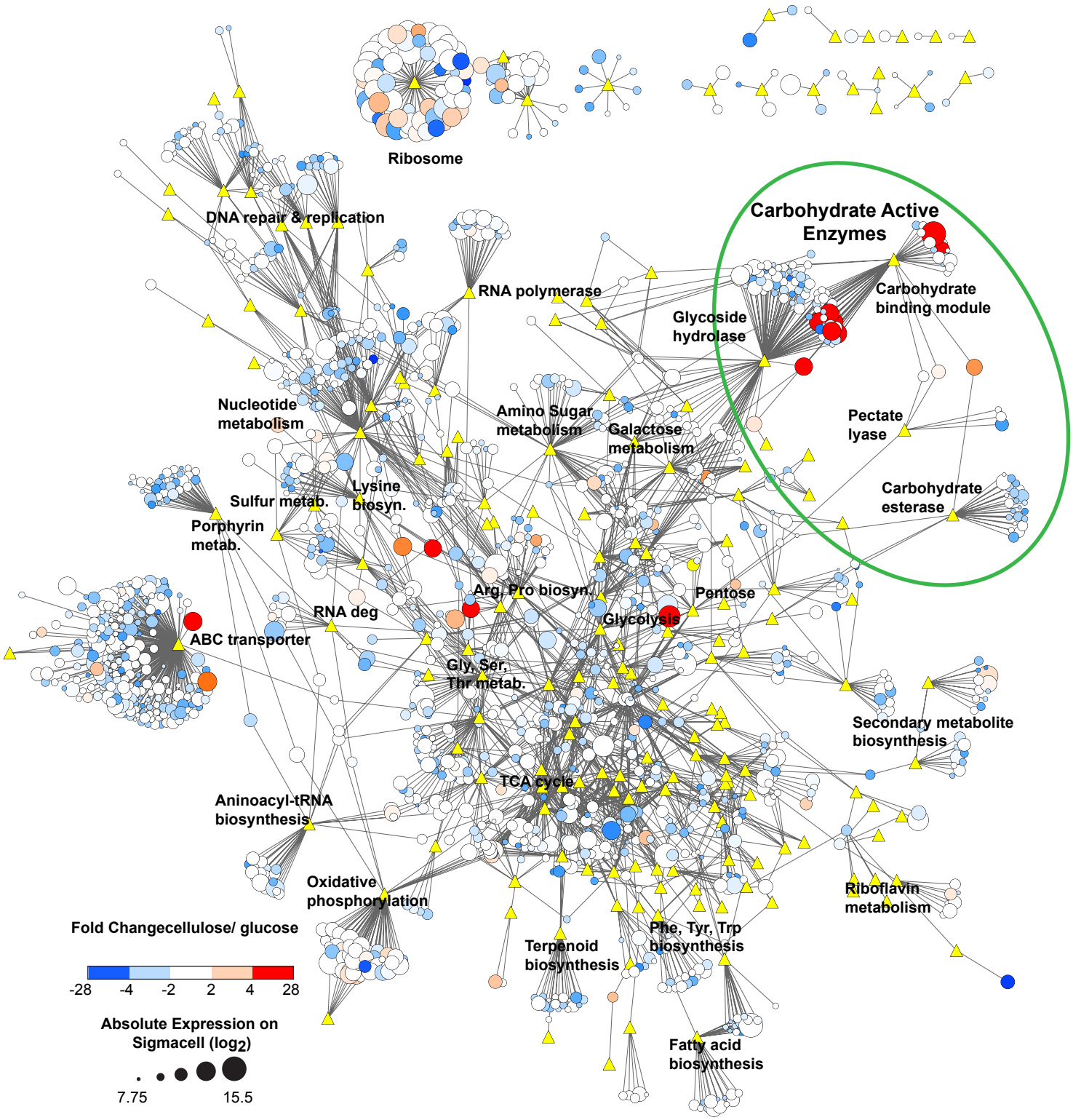
Ribosome
DNA repair & replication
RNA polymerase
Carbohydrate Active Enzymes
Carbohydrate binding module
Glycoside hydrolase
Nucleotide metabolism
Amino Sugar metabolism
Galactose metabolism
Pectate lyase
Carbohydrate esterase
Lysine biosyn.
Sulfur metab.
Porphyrin metab.
Arg, Pro biosyn.
Pentose
Glycolysis
RNA deg
ABC transporter
Gly, Ser, Thr metab.
Secondary metabolite biosynthesis
TCA cycle
Aninoacyl-tRNA biosynthesis
Oxidative phosphorylation
Riboflavin metabolism
Phe, Tyr, Trp biosynthesis
Terpenoid biosynthesis
Fatty acid biosynthesis
Fold Changecellulose/ glucose
-28 -4 -2 2 4 28
Absolute Expression on Sigmacell (log2)
7.75 15.5

Figure S6

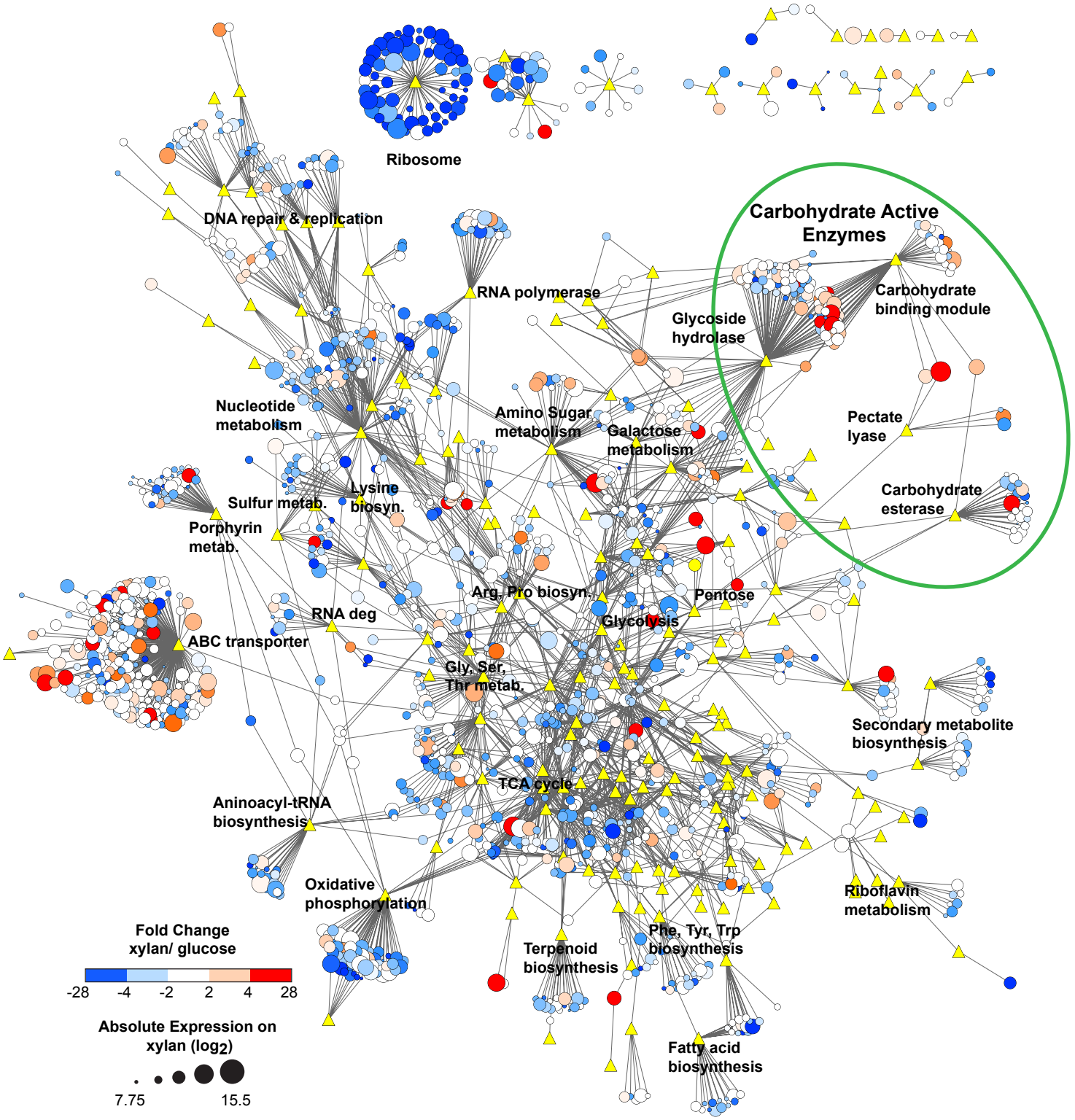
Ribosome
DNA repair & replication
RNA polymerase
Carbohydrate Active Enzymes
Carbohydrate binding module
Glycoside hydrolase
Nucleotide metabolism
Amino Sugar metabolism
Galactose metabolism
Pectate lyase
Carbohydrate esterase
Lysine biosyn.
Sulfur metab.
Porphyrin metab.
Arg, Pro biosyn.
Pentose
Glycolysis
RNA deg
ABC transporter
Gly, Ser, Thr metab.
Secondary metabolite biosynthesis
TCA cycle
Aninoacyl-tRNA biosynthesis
Oxidative phosphorylation
Riboflavin metabolism
Phe, Tyr, Trp biosynthesis
Terpenoid biosynthesis
Fatty acid biosynthesis
Fold Change xylan/ glucose
-28 -4 -2 2 4 28
Absolute Expression on xylan (log2)
7.75 15.5

Figure S7

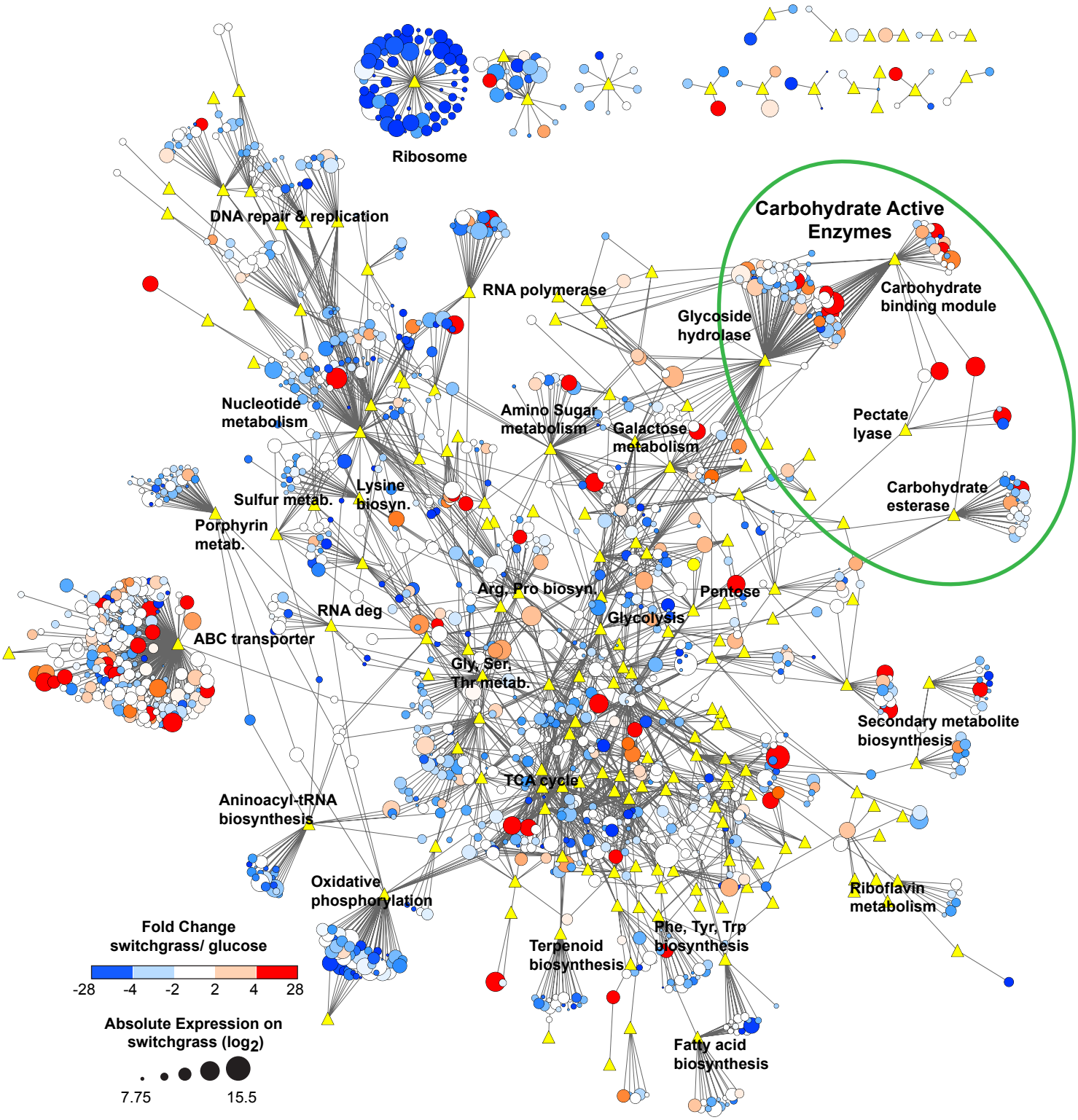
Ribosome
DNA repair & replication
RNA polymerase
Carbohydrate Active Enzymes
Carbohydrate binding module
Glycoside hydrolase
Nucleotide metabolism
Amino Sugar metabolism
Galactose metabolism
Pectate lyase
Carbohydrate esterase
Lysine biosyn.
Sulfur metab.
Porphyrin metab.
Arg, Pro biosyn.
Pentose
Glycolysis
RNA deg
ABC transporter
Gly, Ser, Thr metab.
Secondary metabolite biosynthesis
TCA cycle
Aninoacyl-tRNA biosynthesis
Oxidative phosphorylation
Riboflavin metabolism
Phe, Tyr, Trp biosynthesis
Terpenoid biosynthesis
Fatty acid biosynthesis
Fold Change switchgrass/ glucose
-28 -4 -2 2 4 28
Absolute Expression on switchgrass (log2)
7.75 15.5

Figure S8

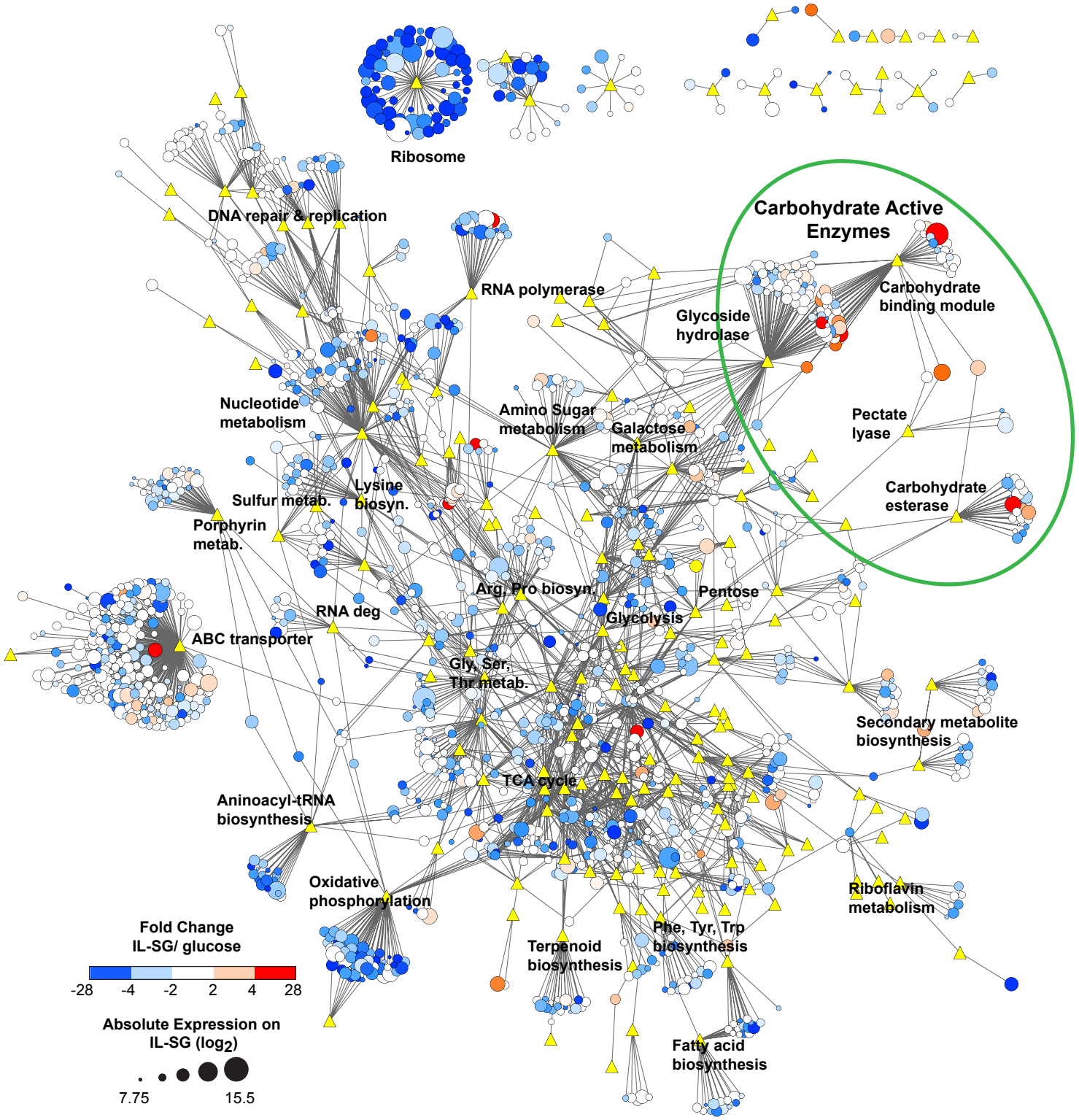
Ribosome
DNA repair & replication
RNA polymerase
Carbohydrate Active Enzymes
Carbohydrate binding module
Glycoside hydrolase
Nucleotide metabolism
Amino Sugar metabolism
Galactose metabolism
Pectate lyase
Carbohydrate esterase
Lysine biosyn.
Sulfur metab.
Porphyrin metab.
Arg, Pro biosyn.
Pentose
Glycolysis
RNA deg
ABC transporter
Gly, Ser, Thr metab.
Secondary metabolite biosynthesis
TCA cycle
Aninoacyl-tRNA biosynthesis
Oxidative phosphorylation
Riboflavin metabolism
Terpenoid biosynthesis
Phe, Tyr, Trp biosynthesis
Fatty acid biosynthesis
Fold Change IL-SG/ glucose
-28
-4
-2
2
4
28
Absolute Expression on IL-SG (log2)
7.75
15.5

Figure S9

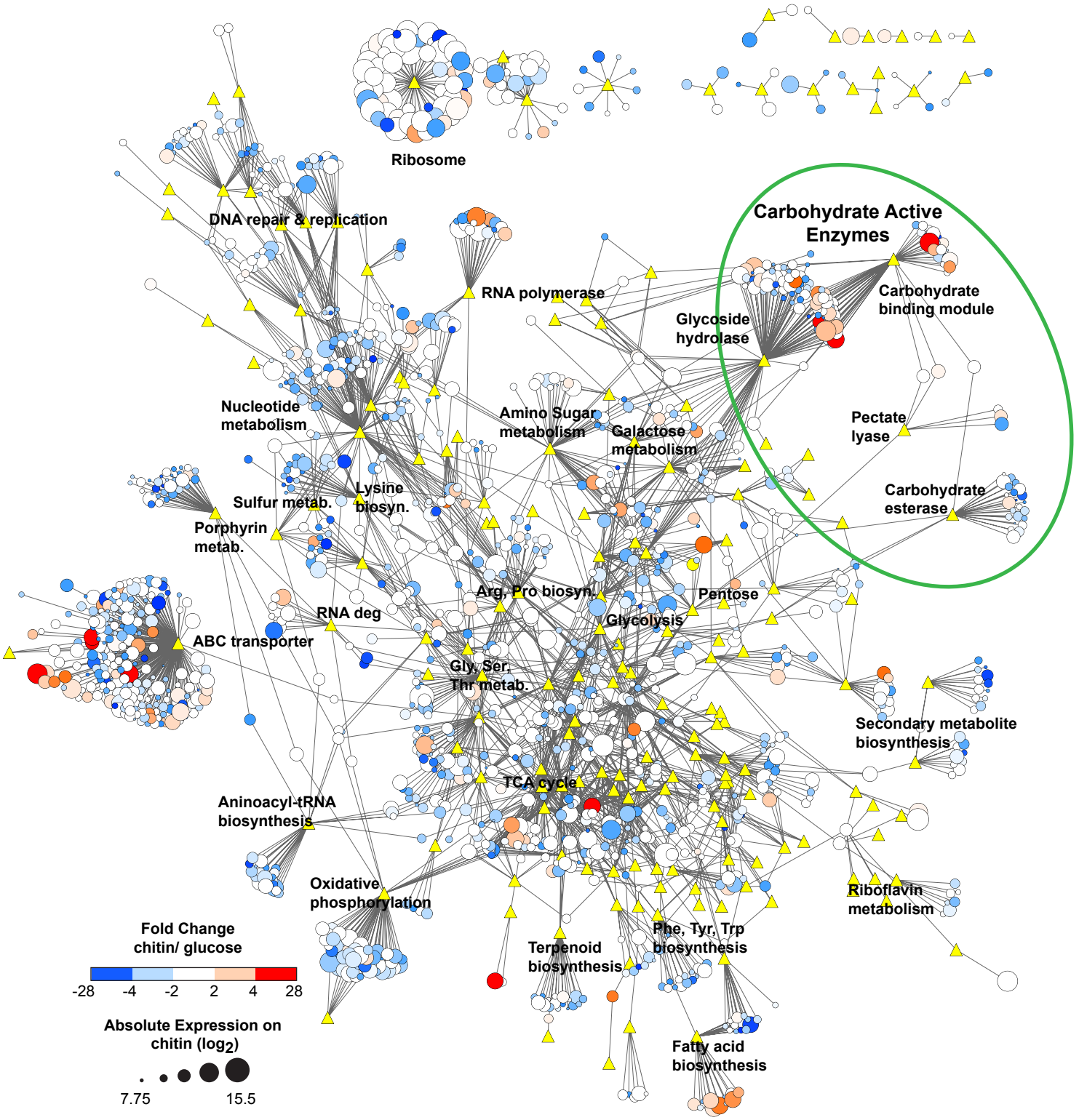
Ribosome
DNA repair & replication
RNA polymerase
Carbohydrate Active Enzymes
Carbohydrate binding module
Glycoside hydrolase
Nucleotide metabolism
Amino Sugar metabolism
Galactose metabolism
Pectate lyase
Carbohydrate esterase
Lysine biosyn.
Sulfur metab.
Porphyrin metab.
Arg, Pro biosyn.
Pentose
Glycolysis
RNA deg
ABC transporter
Gly, Ser, Thr metab.
Secondary metabolite biosynthesis
TCA cycle
Aninoacyl-tRNA biosynthesis
Oxidative phosphorylation
Riboflavin metabolism
Phe, Tyr, Trp biosynthesis
Terpenoid biosynthesis
Fatty acid biosynthesis
Fold Change chitin/ glucose
-28 -4 -2 2 4 28
Absolute Expression on chitin (log2)
7.75 15.5

Figure S10

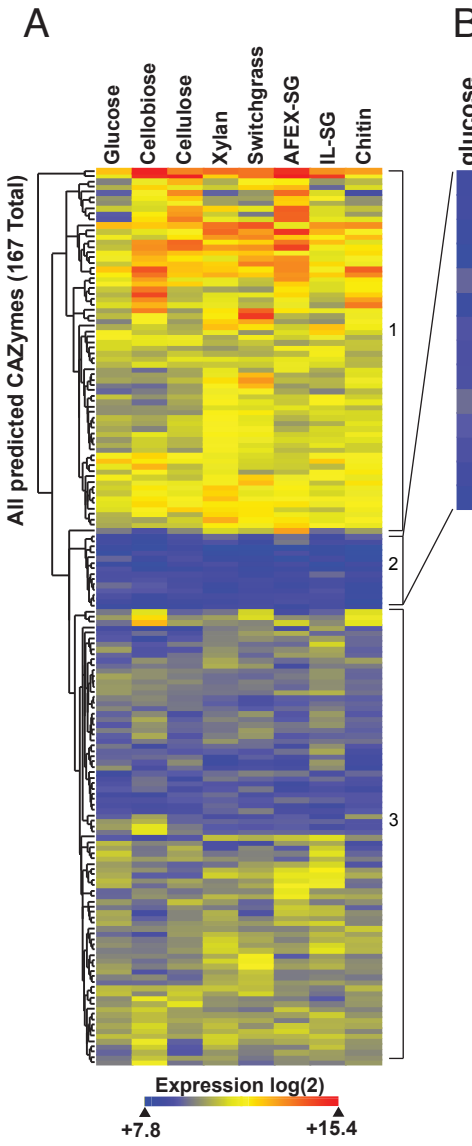

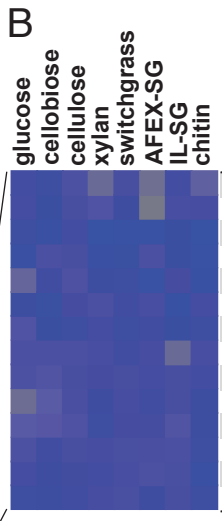

Locus	CAZy	Function
SACTE_0860	GH18	Glycoside hydrolase, family 18
SACTE_0531	GH3	Glycoside hydrolase, family 3
SACTE_4356	CE14	N-acetylglucosaminyl phosphatidylinositol deacetylase
SACTE_0483	CBM2	Cellulose-binding domain, family II
SACTE_5949	CE4	Glycoside hydrolase/deacetylase
SACTE_5252	CE12	Esterase, SGNH hydrolase-type, subgroup
SACTE_3168	GH65	Six-hairpin glycosidase-like
SACTE_5458	GH46	Glycoside hydrolase, family 46
SACTE_6011	GH27	Glycoside hydrolase, family 27
SACTE_1814	GH0	Six-hairpin glycosidase-like
SACTE_0303	CE4	Glycoside hydrolase/deactylase
SACTE_1602	GH114	TM1410 hypothetical-related protein
SACTE_1311	CE8	Pectinesterase
SACTE_0094	CE4	Putative urate catabolism protein

Figure S11

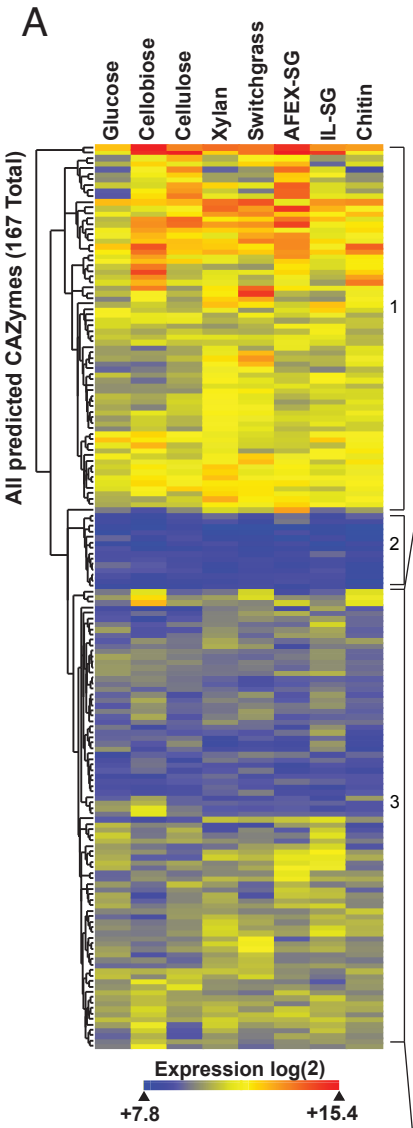

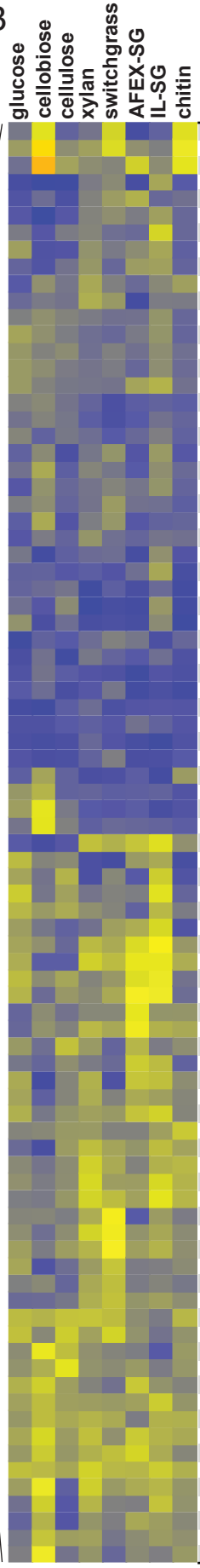

Locus	CAZy	Function
SACTE_6493	CBM33	Chitin-binding, domain 3
SACTE_4246	GH18	Galactose-binding domain-like
SACTE_0080	CBM33	Chitin-binding, domain 3
SACTE_6203	CE4	Glycoside hydrolase/deacetylase, beta/alpha-barrel
SACTE_6512	CBM13	Cadherin-like
SACTE_1291	GH42,43	Beta-galactosidase C-terminal
SACTE_4322	GH65	Galactose-binding domain-like
SACTE_4336	CE7	Acetyl xylan esterase
SACTE_1161	CBM33	Chitin-binding, domain 3
SACTE_5764	GH18	Carbohydrate-binding domain, family 5/12
SACTE_5267	GH43	Twin-arginine translocation pathway, signal sequence
SACTE_4719	GH3	Glycoside hydrolase, family 3, C-terminal
SACTE_5629	GH93	Ricin B lectin
SACTE_5315	GH13	Glycosyl hydrolase, family 13, catalytic domain
SACTE_4708	CBM35	Soluble quinoprotein glucose/sorbosone dehydrogenase
SACTE_3047	CE10	Six-bladed beta-propeller, TolB-like
SACTE_5843	GH4	Glycoside hydrolase, family 4
SACTE_4649	GH13	Immunoglobulin-like fold
SACTE_2871	CBM12	Intradiol ring-cleavage dioxygenase, core
SACTE_5680	CE10	Peptidase S9, prolyl oligopeptidase, catalytic domain
SACTE_5673	CE4	Glycoside hydrolase/deacetylase, beta/alpha-barrel
SACTE_5226	GH1	Glycoside hydrolase, family 1
SACTE_5875	GH23	hypothetical protein
SACTE_2087	GH4	Glycoside hydrolase, family 4
SACTE_0549	GH16	Concanavalin A-like lectin/glucanase
SACTE_6261	CE14	N-acetylglucosaminyl phosphatidylinositol deacetylase
SACTE_5461	GH5	Glycoside hydrolase, family 5
SACTE_5460	GH3	Glycoside hydrolase, family 3, C-terminal
SACTE_2080	GH84	Galactose-binding domain-like
SACTE_0562	GH74	Cellulose-binding family II/chitobiase, carbohydrate-binding domain
SACTE_5800	CE8	Pectinesterase, catalytic
SACTE_2290	CBM2	Cellulose-binding domain, family II, bacterial type
SACTE_2078	GH77	Glycoside hydrolase, family 77
SACTE_0561	GH43	Glycoside hydrolase, family 43
SACTE_2876	GH16	Ricin B lectin
SACTE_0367	GH42,43	Beta-galactosidase C-terminal
SACTE_1901	GH51	Alpha-L-arabinofuranosidase, C-terminal
SACTE_0095	GH16	Concanavalin A-like lectin/glucanase
SACTE_1310	PL3	Pectate lyase, catalytic
SACTE_1205	GH15	Six-hairpin glycosidase-like
SACTE_2232	GH3	Glycoside hydrolase, family 3, C-terminal
SACTE_0092	GH0	Neuraminidase
SACTE_5816	GH31	Glycoside hydrolase, family 31
SACTE_3544	CBM51	RNA polymerase sigma factor, region 3/4
SACTE_5319	GH13	Malto-oligosyltrehalose synthase
SACTE_5159	GH43	Glycoside hydrolase, family 43
SACTE_0383	GH92	Alpha-1,2-mannosidase, putative
SACTE_5592	GH114	TM1410 hypothetical-related protein
SACTE_5271	CE4	Glycoside hydrolase/deacetylase, beta/alpha-barrel
SACTE_3065	GH19	Glycoside hydrolase, family 19
SACTE_1313	CE12	Lipase, GDSL
SACTE_0528	GH115	Twin-arginine translocation pathway, signal sequence
SACTE_6517	GH35	Glycoside hydrolase, family 35
SACTE_4730	GH30	Ricin B lectin
SACTE_1257	GH15	Six-hairpin glycosidase-like
SACTE_1315	GH43	Glycoside hydrolase, family 43
SACTE_6394	CE14	N-acetylglucosaminyl phosphatidylinositol deacetylase
SACTE_4332	GH1	Glycoside hydrolase, family 1
SACTE_0133	CBM35,6	Galactose-binding domain-like
SACTE_6494	GH18	Glycoside hydrolase, chitinase active site
SACTE_5372	CBM40	Lipase, GDSL
SACTE_5235	GH92	Galactose-binding domain-like
SACTE_5815	GH3	Galactose-binding domain-like
SACTE_0359	GH13	Glycosyl hydrolase, family 13, subfamily, catalytic domain
SACTE_5685	GH13	Glycoside hydrolase, subgroup, catalytic core
SACTE_6462	CBM42	RNA polymerase sigma factor, region 2
SACTE_5373	CE7	Acetyl xylan esterase
SACTE_5811	GH42,43	Beta-galactosidase C-terminal
SACTE_5628	GH2	Galactose-binding domain-like
SACTE_0311	GH0	Glycoside hydrolase, subgroup, catalytic core
SACTE_3141	CE14	N-acetylglucosaminyl phosphatidylinositol deacetylase
SACTE_1647	GH13	Glycosyl hydrolase, family 13, subfamily, catalytic domain
SACTE_2439	CE4	Glycoside hydrolase/deacetylase, beta/alpha-barrel
SACTE_1422	GH23	Twin-arginine translocation pathway, signal sequence
SACTE_4212	CE14	Mycothiol conjugate amidase, Mca
SACTE_6015	GH36	Glycoside hydrolase, family 36
SACTE_5809	GH12	Concanavalin A-like lectin/glucanase
SACTE_5886	GH46	Glycoside hydrolase, family 46
SACTE_5183	CBM13	Ricin B lectin
SACTE_5065	CE4	Glycoside hydrolase/deacetylase, beta/alpha-barrel
SACTE_0366	GH78	Six-hairpin glycosidase-like
SACTE_5418	GH23	Peptidoglycan binding-like
SACTE_0379	GH2	Galactose-binding domain-like
SACTE_4739	GH3	Na-Ca exchanger/integrin-beta4
SACTE_0076	GH114	TM1410 hypothetical-related protein

Table S1 : Proteins separated by ion exchange chromatography and identified by mass spectrometry.

Protein band[a]	Locus	Catalytic domain	CBM	Functional class[b]
a	SACTE_3159	CBM33	CBM2	cellulase
b	SACTE_0265	GH10	CBM2	xylanase
c	SACTE_4755	GH64		beta-1,3-glucanase
d	SACTE_0482	GH5	CBM2	cellulase
e	SACTE_0237	GH6	CBM2	cellulase
f	SACTE_0236	GH48	CBM2	cellulase
g	SACTE_3717	GH9	CBM2	cellulase
h	SACTE_2347	GH5	CBM2	mannanase

[a] Protein bands labeled in Figure 3A were identified by MALDI-TOF mass spectrometry. [b] Function identified by assays of individual fractions from ion exchange chromatography.